Effect of magnetic field on the boundary layer flow, heat, and mass transfer of nanofluids over a stretching cylinder

Aminreza Noghrehabadi[*], Mohammad Ghalambaz, Ehsan Izadpanahi, Rashid Pourrajab

Department of Mechanical Engineering, Shahid Chamran University of Ahvaz, Ahvaz, Iran

A B S T R A C T

The effect of a transverse magnetic field on the boundary layer flow and heat transfer of an isothermal stretching cylinder is analyzed. The governing partial differential equations for the magnetohydrodynamic, temperature, and concentration boundary layers are transformed into a set of ordinary differential equations using similarity transformations. The obtained ordinary differential equations are numerically solved for a range of non-dimensional parameters. Results show that the presence of a magnetic field would significantly affects the boundary layer profiles. An increase in magnetic parameter would decrease the reduced Nusselt and Sherwood numbers.

1. Introduction

Recently, a number of studies have been carried out on the effects of electrically conducting fluids on the flow and heat transfer of a viscous fluid passing a moving surface in the presence of a magnetic field. Liquid metals and water mixed with a little acid are the two common examples of electrically conducting liquids. There are some examples about technological applications of magnetohydrodynamic (MHD) viscous flow which include hot rolling, wire drawing, annealing, thinning of copper wires, glass-fiber and paper production, drawing of plastic films, metal and polymer extrusion, and metal spinning. In all these cases, the properties of the final product depend on the rate of cooling by drawing such strips in electrically conducting fluids subject to a magnetic field. Therefore, the heating or cooling characteristics during such processes have a significant influence on the quality of the final products. The heating or cooling characteristics mostly depend on the skin friction and the surface heat transfer rate.

Common heat transfer fluids such as water, ethylene glycol, and engine oil have limited heat transfer capabilities owing to their low thermal conductivity, whereas metals have much higher thermal conductivities than these fluids. Therefore, dispersing high thermal conductive solid particles in a conventional heat transfer fluid may enhance the thermal conductivity of the resulting fluid.

Corresponding author: Aminreza Noghrehabadi, Ph.D., Associate Professor at Mechanical Engineering Department, Shahid Chamran University of Ahvaz, Ahvaz, Iran. Email: noghrehabadi@scu.ac.ir, a.r.noghrehabadi@gmail.com, Mobile: +98916 312 8841, Tell: +98 611 3330010 Ext. 5678, Fax: +98 611 3336642

Nanofluid is a fluid containing nanometer-sized particles, called nanoparticles. The term "Nanofluid" has been first proposed by Choi [1] to indicate engineered colloids consist of nanoparticles dispersed in a base fluid. The base fluid is usually a conductive fluid, such as water or ethylene glycol. Other base fluids include bio-fluids, polymer solutions, oils, and other lubricants. One of the outstanding characteristic of nanofluids is their enhanced thermal conductivity [2]. The nanoparticles used in synthesis of nanofluids are typically metallic (Al, Cu), metallic oxides (Al_2O_3, TiO_2), carbides (SiC), nitrides (AlN, SiN) or carbon nanotubes with the diameter which ranges between 1 and 100 nm. The thermophoresis and Brownian motion effects are also important in heat transfer of nanofluids. The migration of nanoparticles because of these effects would influence the local heat transfer rate.

Recently, the flow and heat transfer over stretching surfaces have attracted the attention of many researchers [3-6].

Ishak et al. [7] investigated the magnetohydrodaynamic flow and heat transfer over a stretching cylinder. They reduced the governing equations to a system of ordinary differential equations. Later, the system of equations was numerically solved using Keller box method. The effect of magnetic parameter, Prandtl number, and Reynolds number on the velocity and temperature fields were thoroughly examined. Wang [8] investigated the steady flow of a viscous fluid outside a stretching hollow cylinder. Ishak et al. [9] studied the effect of suction/blowing on the flow and heat transfer past a stretching cylinder. They found that the magnitude of the skin friction coefficient increases with Reynolds number while the variation of Prandtl number does not show a significant effect on the skin friction coefficient.

Recently, Rasekh et al. [10] have analyzed the flow and heat transfer of nanofluids over a stretching cylinder. They reduced the governing equations to a set of ordinary differential equations. They have reported that the slip of nanoparticles because of thermophoresis and Brownian motion forces affects the heat transfer rate of nanofluids in the boundary layer. Gorla et al. [11] have considered a melting boundary condition on the surface of the stretching cylinder and analyzed the flow and heat transfer of nanofluids.

To the best of author's knowledge, the effect of a magnetic field on the boundary layer flow and heat transfer of nanofluids over a stretching cylinder has not been analyzed yet. The present study aims to analyze the development of the steady boundary layer flow and heat transfer of a magnetohydrodynamic nanofluid over a stretching cylinder. The governing partial differential boundary layer equations in the cylindrical form are presented and then transformed into a set of ordinary differential equations. The obtained equations are a function of magnetic parameter M, suction/injection parameter γ, Reynolds number Re, Prandtl number Pr, Lewis number Le, Brownian motion parameter Nb, and thermophoresis parameter Nt. The equations are solved numerically for a range of non-dimensional parameters.

2. Formulation of the problem

Consider the laminar steady flow of an incompressible electrically conducting nanofluid (with electrical conductivity σ) over a linear stretching cylinder. The movement of flow is because of the stretch of the cylinder. The flow outside the boundary layer is quiescent. A uniform magnetic field of intensity B_0 acts in the radial direction. It is assumed that the effect of the induced magnetic field is negligible, which is valid when the magnetic Reynolds number is small. The viscous dissipation, Ohmic heating, and Hall effects are neglected as they are also assumed to be small. Fig. 1 depicts a schematic view of the physical model and the coordinate system. z-axis is measured along the axis of the cylinder and the r-axis is measured in the radial direction. The axial velocity of the stretching cylinder was assumed to be linear. Hence, it can be represented as $w_w = 2c.z$ where c is a positive constant. The surface of the stretching cylinder is permeable; therefore, the surface of the cylinder is subject to mass transfer, which can be represented as $u_w = -c.a.\gamma$. The positive and negative values of γ show mass absorption and mass injection, respectively. The temperature and concentration of nanofluid outside the boundary layer are constant values of T_w and φ_w. The thermo-physical properties are assumed to be constant. Under such assumptions, the governing equation for conservation of mass, momentum, thermal energy, and nanoparticles' concentration are as following:

$$\frac{\partial(rw)}{\partial z} + \frac{\partial(ru)}{\partial r} = 0 \tag{1}$$

$$w\frac{\partial w}{\partial z} + u\frac{\partial w}{\partial r} = \nu\left(\frac{\partial^2 w}{\partial r^2} + \frac{1}{r}\frac{\partial w}{\partial r}\right) - \frac{\sigma B_0^2}{\rho}w \tag{2}$$

$$w\frac{\partial u}{\partial z} + u\frac{\partial u}{\partial r} = -\frac{1}{\rho}\frac{\partial p}{\partial r} + \nu\left(\frac{\partial^2 u}{\partial r^2} + \frac{1}{r}\frac{\partial u}{\partial r} - \frac{u}{r^2}\right) \tag{3}$$

$$w\frac{\partial T}{\partial z} + u\frac{\partial T}{\partial r} = \alpha\frac{1}{r}\frac{\partial}{\partial r}\left(r\frac{\partial T}{\partial r}\right) +$$

$$\tau\left\{D_B\left(\frac{\partial T}{\partial r}\frac{\partial C}{\partial r}\right) + \frac{D_T}{T_\infty}\left(\frac{\partial T}{\partial r}\right)^2\right\} \tag{4}$$
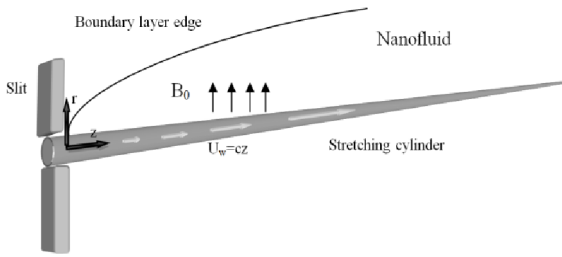
Fig. 1. Physical model and coordinate system.

$$w\frac{\partial C}{\partial z}+u\frac{\partial C}{\partial r}=D_B\frac{1}{r}\frac{\partial}{\partial r}\left(r\frac{\partial C}{\partial r}\right)+$$
$$\left(\frac{D_T}{T_\infty}\right)\left(\frac{1}{r}\frac{\partial}{\partial r}\left(r\frac{\partial T}{\partial r}\right)\right)\tag{5}$$

here u and w are the velocity components along the r and z axes, respectively. p is the fluid pressure, ρ is the density of nanofluid, v is the kinematic viscosity of nanofluid, σ is the electrical conductivity of nanofluid and B_0 is the strength of the uniform magnetic field, α is the thermal diffusivity of nanofluid, D_B is the Brownian diffusion coefficient, D_T is the thermophoresis diffusion coefficient. τ is the ratio between the effective heat capacity of the nanoparticles $((\rho c)p)$ and heat capacity of the nanofluid $((\rho c)_{nf})$, i.e. $\tau = (\rho c)_p /(\rho c)_{nf}$.

The boundary conditions on the surface of the cylinder are:

$$w = w_w = 2cz\,, \quad u = -ca\gamma,$$
$$T = T_w\,, \quad C = C_w \qquad\qquad at\ \ r = a \tag{6}$$

where c is a constant and z is the axial direction. The appropriate boundary conditions at the far field (i.e. $r\rightarrow\infty$) are:

$$w = 0, \qquad T = T_\infty\,, \qquad C = C_\infty \tag{7}$$

Introducing the following similarity variables reduces the governing and boundary conditions to the set of ordinary differential equations (Eqs. 9-11) subjected to boundary conditions 12 and 13:

$$\eta = \left(\frac{r}{a}\right)^2,u = -ca\left(\frac{f(\eta)}{\sqrt{\eta}}\right),\tag{8-a}$$
$$w = 2cf'(\eta)z\,,$$
$$\phi(\eta) = \frac{C - C_\infty}{C_w - C_\infty}, \quad \theta(\eta) = \frac{T - T_\infty}{T_w - T_\infty}\tag{8-b}$$
$$\eta f''' + f'' - Re(f'^2 - ff'') - Mf' = 0\tag{9}$$
$$\eta\theta'' + Pr\,\eta\theta'\left(Nb\phi' + Nt\theta'\right) + \left(1 + Pr\,Re\,f\right)\theta' = 0\tag{10}$$

$$\eta\phi'' + \frac{Nt}{Nb}\left(\eta\theta'' + \theta'\right) + \left(1 + Re\,Le\,f\right)\phi' = 0\tag{11}$$

$$At\ \eta = 1 \quad : \quad f = \gamma, \quad f' = 1, \quad \theta = 1, \quad \phi = 1\tag{12}$$

$$At\ \eta \rightarrow \infty \quad : \quad f' = 0, \quad \theta = 0, \quad \phi = 0\tag{13}$$

The parameters in Eqs. (9)-(11) are defined as:

$$Pr = \frac{v}{\alpha}, \quad Re = \frac{ca^2}{2v}, \quad Le = \frac{v}{D_B}, \quad M = \frac{\sigma B_0^2 a^2}{4v\rho}\tag{14}$$
$$Nb = \frac{\tau D_B(C_w - C_\infty)}{v}\,, \quad Nt = \frac{\tau D_T(T_w - T_\infty)}{v T_\infty}\tag{15}$$

here Pr, Re, Le, M, Nb and Nt denote the Prandtl number, Reynolds number, Lewis number, the magnetic parameter, the Brownian motion parameter, and the thermophoresis parameter, respectively. The pressure P also can be determined from Eq. (3) as following:

$$\frac{p - p_\infty}{\rho cv} = -\frac{Re}{\eta}f^2(\eta) - 2f'(\eta)\tag{16}$$

Physical quantities of interest are the skin friction coefficient C_f, Nusselt number Nu, and Sherwood number Sh, which can be defined as:

$$C_f = \frac{\tau_w}{\rho w_w^2 / 2}, \quad Nu = \frac{aq_w}{k(T_w - T_\infty)}, \quad Sh = \frac{am_w}{D_B(C_w - C_\infty)}\tag{17}$$

where τ_w is the wall shear stress, q_w is the wall heat flux, and m_w is the nanoparticle mass flux from the surface of the tube, given as:

$$\tau_w = \mu\left(\frac{\partial w}{\partial r}\right)_{r=a}, \quad q_w = -k\left(\frac{\partial T}{\partial r}\right)_{r=a}, \quad m_w = -D_B\left(\frac{\partial C}{\partial r}\right)_{r=a}\tag{18}$$

Using similarity variables the non-dimensional skin friction coefficient, Nusselt number, and Sherwood number are obtained as:

$$c_f(Re\,z / a) = f''(1)\,, \quad Nu = -2\theta'(1), \quad Sh = -2\phi'(1)\tag{19}$$

To estimate the accuracy of the present results, an error analysis should be considered. For this purpose the error percentage is introduced as:

$$error = \left(\left|\frac{\chi_{present} - \chi_{ishak\ et\ al.[7]}}{\chi_{ishak\ et\ al.[7]}}\right|\right)\times 100\tag{20}$$

here, X could be any quantity such as $f''(1)$, $\theta'(1)$, or etc.

3. Results and discussion

The ordinary differential equations, Eqs. (9)-(11), subject to the boundary conditions, Eqs. (12) and (13), are numerically solved using the forth-order Rung-Kutta and Newton-Raphson method [12] with a systematic guessing of $f''(1)$, $\theta'(1)$, and $\Phi'(1)$ using the shooting technique. The step size $\Delta\eta= 0.001$ is used for calculations. The computations were done using Fortran 90.

By neglecting the effects of thermophoresis and Brownian motion, the present study reduces to the case of a pure fluid, which was studied by Ishak [7]. Therefore, the results reported by Ishak [7] are used to evaluate the accuracy of the present solution. Table 1 shows a comparison between the present results and those reported by Ishak [7] for different values of magnetic parameter when Re=10 and Pr=7.0. Table 1 shows excellent agreement between the results of present study and the results reported by Ishak [7].

In the present study, the values of magnetic parameter (M) are chosen $0 < M < 5$ to clearly show the effect of this parameter on the dimensionless velocity, temperature and concentration profiles as well as the Nusselt number. Most nanofluids reported in the literatures have large values of Lewis number, i.e., $Le > 1$ [13-15]. Hence, the values of Lewis number are chosen $2<Le<10$. The same values of Nb, and Nt as those adopted by Rasekh et al. [10] and Gorla et al. [11] are used in the present study. The latter values ,compared to the previous studies, allow us to evaluate the effect of magnetic fields.

Fig. 2 exhibits the effect of magnetic parameter (M) on the velocity profiles. The maximum value of velocity is at the surface of the cylinder, and then the velocity decreases
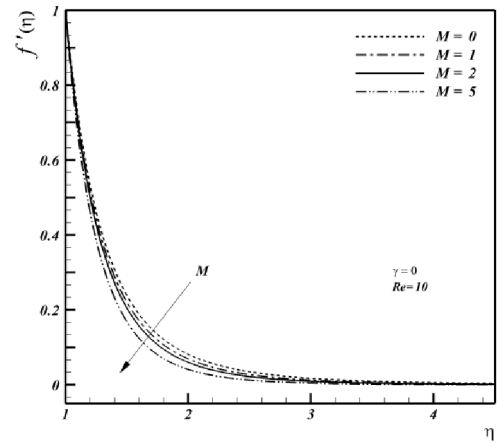
Fig. 2. Effect of magnetic parameter on the velocity profiles.

asymptotically to zero far from the stretching surface. The velocity profiles decrease as the magnetic parameter increases. The increase of magnetic parameter increases the induced Lorentz force in the boundary layer, and hence, it decreases the velocity profiles in the boundary layer. This indicates the fact that an increase in the magnetic parameter would increases the Lorentz force, and consequently, an augmentation of the Lorenz force opposes the flow and reduces the fluid motion. However, variation of magnetic parameter does not show significant effect on the thickness of hydraulic boundary layer.

Fig. 3 depicts the effect of magnetic parameter on temperature profiles. This figure shows that the temperature profiles increase as the magnetic parameter

Table 1: Comparison of results for the skin friction coefficient $f''(1)$ and the reduced Nusselt number $-\theta'(1)$ for several values of M for $Re = 10$, Pr=7 and $Nt = Nb = 0$.

M	$-f''(1)$			$-\theta'(1)$		
	Current result	Ishak et al. [7]	Error percent	Current result	Ishak et al. [7]	Error percent
0.00	3.44448	3.4444	2.3E-03	6.1579	6.1592	2.1E-02
0.01	3.34617	3.3461	2.1E-03	6.1575	6.1588	2.1E-02
0.05	3.35291	3.3528	3.3E-03	6.1560	6.1583	3.7E-02
0.10	3.36131	3.3612	3.2E-03	6.1541	6.1554	2.1E-02
0.50	3.42743	3.4274	8.8E-04	6.1390	6.1402	2.0E-02
1.00	3.50769	3.5076	2.6E-03	6.1207	6.1219	2.0E-02
2.00	3.66154	3.6615	1.1E-03	6.0857	6.0864	1.1E-02
5.00	4.08263	4.0825	3.2E-03	5.9899	5.9895	6.7E-03

increases. Indeed, the increase of magnetic parameter reduces the magnitude of velocity profiles in the boundary layer, and hence, the temperature in the boundary layer would rise. The variation of magnetic parameter does not show significant effect on the thickness of thermal boundary layer past the stretching cylinder. Fig. 4 illustrates the effect of magnetic parameter on the concentration profiles. As it can be seen, the increase of magnetic parameter increases the magnitude of concentration profiles. As mentioned, increase of magnetic parameter reduces the magnitude of velocity profiles in the boundary layer. Therefore, the decrease of velocity in the boundary layer induces the diffusion of nanoparticles in the boundary layer. However, on the other hand, increase of magnetic parameter tends to decrease the temperature gradients in the boundary layer (as what was seen in Fig. 3). In nanofluids, the thermophoresis force acts opposite to the temperature gradient and tends to move nanoparticles from hot to cold. The magnitude of thermophoresis is proportional to the temperature gradient [16]. Therefore, a decrease in the temperature gradient decreases the effect of thermophoresis in the boundary layer, and consequently tends to decrease the diffusion of nanoparticles. Fig. 4 demonstrates that as the magnetic parameter increases, the effect of variation of velocity on the concentration profiles is the dominant effect.

Increasing the magnetic parameter increases the Lorentz force which creates the force opposed to the fluid motion. Increasing the Lorentz force decreases the velocity in the boundary layer. Based on the momentum equations, it is clear that the magnetic force corresponds to multiplex of velocity and the magnetic field magnitude. In the present study, the magnetic field was assumed to be comparatively high and uniform in the boundary layer.
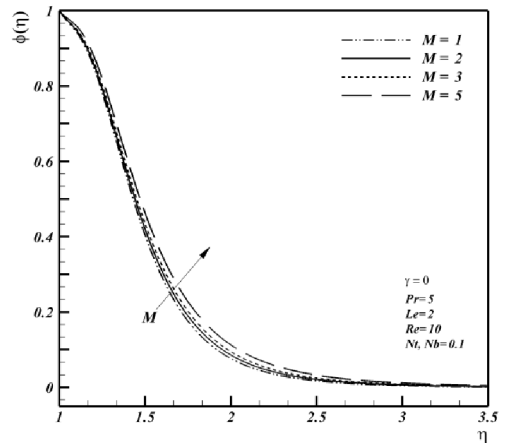
Fig. 4. Effect of magnetic parameter on concentration profiles.

Thus, the magnetic force is solely a function of velocity of the fluid in the boundary layer. It should be noticed that the velocity in the boundary layer is because of the stretching of the cylinder. Consequently, the maximum velocity can be observed on the surface of the cylinder while the minimum velocity is zero which is the quiescent part of the fluid far from the surface (near the edge of the boundary layer). As a result, the maximum magnitude of induced Lorentz force can be seen in the vicinity of the cylinder (this is where the magnetic field strongly affects the velocity and consequently temperature profiles). Far from the surface of the cylinder, the velocities are very low, and consequently, the induced Lorentz force is also very low. Hence, as it can be seen in the figures, the effect of magnetic field is negligible on the thickness of the boundary layer.

Figs. 5 and 6 depict the effect of magnetic parameter on the Nusselt number for selected values of thermophoresis and Brownian motion parameters. These figures show that the Nusselt number is a decreasing function of the magnetic parameter. This observation is in good agreement with Fig. 3. As it was mentioned, the increase in magnetic parameter tends to decrease temperature gradients in the boundary layer and hence decreases the Nusselt number. Figs. 5 and 6 also show that the Nusselt number is a decreasing function of the thermophoresis and Brownian motion parameters. The Brownian motion effect tends to move the nanoparticles from high concentration areas to low ones. Therefore, in the present study, both of the Brownian motion and thermophoresis effects tend to move the nanoparticles away from the stretching cylinder. Indeed, the augmentation of Brownian motion or thermophoresis parameters intensifies the diffusion of

Fig. 3. Effect of magnetic parameter on the temperature profiles.
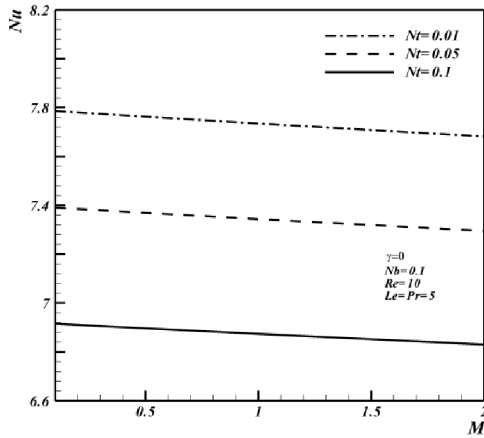
Fig. 5. Effects of Nt and M on the Nusselt number.
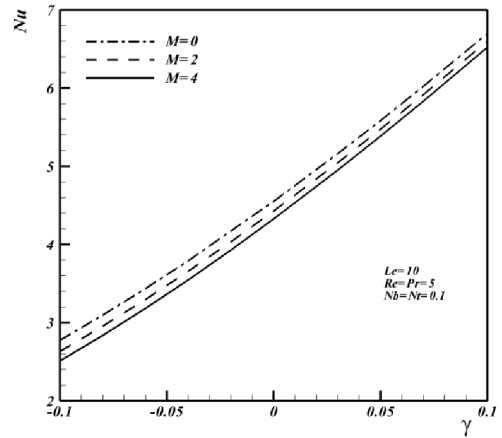
Fig. 7. Effects of M and γ on Nusselt number.
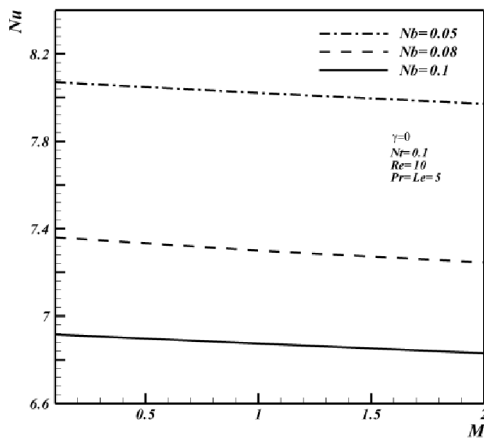
Fig. 6. Effects of Nb and M on Nusselt number.

nanoparticles into the boundary layer and consequently decreases the Nusselt number.

Fig. 7 shows the effect of suction/injection parameter on the Nusselt number for various values of magnetic parameter. This figure shows that the reduced Nusselt number is an increasing function of suction/injection parameter. However, it is a decreasing function of the magnetic parameter. It is noticed from Fig. 7 that the Nusselt number is significantly affected by suction/injection parameter. The positive and negative values of γ indicate mass suction and mass injection, respectively. By increasing the suction, i.e. increase in the magnitude of $\gamma > 0$, the thickness of termal boundary layer decreases, and hence, the temperature gradient at the surface of the cylinder (Nusselt number) increases. This is due to the fact that increasing the suction would bring a large amount of ambient fluid into the surface of the

cylinder. In contrast, increasing the mass injection would percolate the fluid through the boundary layer which can increase the thickness of temperature boundary layer, and hence, the temperature gradient at the surface of the cylinder decreases.

The Nusselt number includes the ratio between convective heat transfer coefficient and conduction heat transfer coefficient (i.e. $Nu=h_{nf}a/k_{nf}$). The experiments demonstrate that dispersing nanoparticles would significantly augment the thermal conductivity of the resulting fluid. Therefore, there is an initial significant potential of increasing heat transfer because of the increase in the thermal conductivity of the mixture as $h_{nf} \sim k_{nf}$ in using nanoparticles. Now, the results of the present study indicate that presence of Brownian motion, thermophoresis, and magnetic field would decrease the reduced Nusselt number. If the increase in the thermal conductivity of the mixture because of the presence of nanoparticles be very significant, then an overall convective enhancement can be seen. However, if the increase in the thermal conductivity of the mixture because of the presence of nanoparticles does not be significant, then the overall convective coefficient may be deteriorated.

4. Conclusion

A combined similarity and numerical approaches was utilized to study the effect of magnetic field on the flow, temperature, and concentration profiles in the boundary layer. The effect of non-dimensional parameters on the Nusselt number is analyzed. The results reveal that:

- An increase in the magnetic parameter would decrease the magnitude of velocity profiles, but it would increase the magnitude of temperature and concentration profiles in the boundary layer.

- The variation of magnetic parameter does not show significant effects on the thickness of the boundary layer profiles (i.e. velocity, temperature, and concentration profiles).
- The Nusselt number is a decreasing function of magnetic parameter, Brownian motion, and thermophoresis parameter, but it is an increasing function of the suction/injection parameter.

Based on the results of the present study, it can be concluded that the effect of Brownian motion and thermophoresis on the reduced Nusselt number is significant. As the reduced Nusselt number is a decreasing function of both Brownian motion and thermophoresis parameters, the heat transfer, associated with using nanofluids, may not be as much as the observed enhancement in the thermal conductivity of nanofluids. Therefore, the single phase models, which neglected the Brownian motion and thermophoresis effects, would overestimate the heat transfer rate induced by using nanofluids.

Acknowledgements

Nomenclature

a	radius of the cylinder
B_0	uniform magnetic field
c	constant
C	nanoparticle volume fraction
C_∞	ambient nanoparticle volume fraction
C_w	nanoparticle volume fraction at the stretching cylinder
C_f	skin friction coefficient
D_B	the Brownian diffusion coefficient
D_T	the thermophoresis diffusion coefficient
k	thermal conductivity of nanofluid
Le	Lewis number
M	magnetic parameter
m_w	wall mass flux
Nb	Brownian motion parameter
Nt	thermophoresis parameter
Nu	Nusselt number
p	pressure
p_∞	ambient pressur
Pr	Prandtl number
q_w	wall Heat flux
Re	Reynolds number
Sh	Sherwood number
T	nanofluid temperature
T_∞	ambient nanofluid temperature
T_w	nanofluid temperature at the stretching cylinder
u,w	velocity components along r- and z-axes
u_w	velocity of the stretching cylinder
r,z	Cartesian coordinates (z-axis is aligned along the stretching cylinder and r-axis is normal to it)

Greek

α	thermal diffusivity of nanofluid
$(\rho c)_{nf}$	heat capacity of the nanofluid
$(\rho c)_p$	effective heat capacity of the nanoparticle material
σ	electrical conductivity of nanofluid
η	similarity variable
$\varphi(\eta)$	dimensionless nanoparticle volume fraction
$\theta(\eta)$	dimensionless temperature
ρ	nanofluid density
ρ_p	nanoparticle mass density
v	kinematic viscosity
τ	parameter defined by ratio between the effective heat capacity of the nanoparticle material and heat capacity of the nanofluid
τ_w	wall shear stress

References

[1]. S.U.S. Choi, Enhancing thermal conductivity of fluids with nanoparticles, in: The Proceedings of the 1995 ASME International Mechanical Engineering Congress and Exposition, San Francisco, USA, ASME, FED 231/MD 66, 99-105 (1995).

[2]. H. Masuda and A. Ebata and K. Teramea and N. Hishinuma, Altering the thermal conductivity and viscosity of liquid by dispersing ultra-fine particles, Netsu Bussei, 4, 227-233 (1993).

[3]. T. Fang, and A. Aziz, Viscous Flow with Second-Order Slip Velocity over a Stretching Sheet, Z. Naturforsch., 65a,1087 −1092 (2010).

[4]. T. Hayat, M. Nawaz, Effect of Heat Transfer on Magnetohydrodynamic Axisymmetric Flow Between Two Stretching Sheets, Z. Naturforsch., 65a, 961 −968 (2010).

[5]. A. S. Butt, S. Munawar, A. Ali, and A. Mehmood, Entropy Analysis of Mixed Convective Magnetohydrodynamic Flow of a Viscoelastic Fluid over a Stretching Sheet, Z. Naturforsch., 67a, 451–459 (2012).

[6]. S. Mukhopadhyay, Upper-Convected Maxwell Fluid Flow over an Unsteady Stretching Surface Embedded in Porous Medium Subjected to Suction/Blowing, Z. Naturforsch., 67a, 641–646 (2012).

[7]. A. Ishak and R. Nazar and I. Pop, Magnetohydrodynamic (MHD) flow and heat transfer due to a stretching cylinder, Energy Conv. Manag., 49, 3265-3269 (2008).

[8]. C.Y. Wang, Fluid flow due to a stretching cylinder, Phys. Fluids, 31, 466-468 (1988).

[9]. A. Ishak and R. Nazar and I. Pop, Uniform suction/blowing effect on flow and heat transfer due to a stretching cylinder, Appl. Math. Model, 32, 2059-2066 (2008).

[10]. A. Rasekh and D.D. Ganji and S. Tavakoli, numerical solution for a nanofluid past over a stretching circular cylinder with non-unifom heat source, Frontiers Heat. Mass. Transf. (FHMT), 3, 043003 (2012).

[11]. R. Subba and R. Gorla and A. Chamkha and E. Al-Meshaiei, melting heat transfer in a nanofluid boundary layer on a stretching circular cylinder, J. Naval Arch. Marin. Eng., 9, 1-10 (2012).

[12]. M. Subhas Abel and P.G. Siddheshwar and N. Mahesha, Numerical solution of the momentum and heat transfer equations for a hydromagnetic flow due to a stretching sheet of a non-uniform property micropolar liquid, Appl. Math. Comp., 217, 5895–5909 (2011).

[13]. W.A. Khan and I. Pop, Boundary-layer flow of a nanofluid past a stretching sheet, Int. J. Heat. Mass. Transf., 53, 2477–2483 (2010).

[14]. R. Kandasamy and P. Loganathan and P. Puvi Arasu, Scaling group transformation for MHD boundary-layer flow of a nanofluid past a vertical stretching surface in the presence of suction/injection, Nuclear Eng. Design, 241, 2053-2059 (2011).

[15]. N. Bachok and A. Ishak and I. Pop, Unsteady boundary-layer flow and heat transfer of a nanofluid over a permeable stretching/shrinking sheet, Int. J. Heat. Mass. Transf., 55, 2102-2109 (2012).

[16]. J. Buongiorno, Convective Transport in Nanofluids, J. Heat. Transf., 128, 240-245 (2006).